



1 A Gauss Elimination Method for estimating locations of extrema in gridded data:

2 Applications for Potential Field Data

3 Dung Nguyen Kim^{a,*}, Dung Tran Tuan^{a,b}

4 ^aInstitute of marine geology and geophysics, Vietnam Academy of Science and Technology.

5 ^bGraduate University of Science and Technology, Vietnam Academy of Science and Technology

6 18 Hoang Quoc Viet Street, Cau Giay District, Hanoi City, Vietnam

7 *kimdunggeo@yahoo.com

8

9 **Abstract:**

10 Extrema in gravity measurements can be used to locate geological structures of
11 interest and the boundaries of such structures can be associated with the maxima in the
12 gradients of the gravitational field strength. Finding the extrema of measured geophysical
13 fields measured on the Earth's surface when the data is sparse is challenging. The inferred
14 positions of such extrema are highly model dependent. Polynomial functions of two variables
15 can be fitted to the data. Higher order polynomials typically give more accurate determination
16 of the extrema, but the maximum order of the polynomial is limited by the number of data
17 points. Difficulties are accentuated in the vicinity of boundaries of the existing data. The
18 maximum horizontal gradient method has often been applied in this context. But in that
19 particular construction, quadratic functions are developed in each dimension. Although the
20 magnitudes of the extracted coefficients are obtained from three points related by their
21 positions on orthogonal straight lines, off axis information should be included as well. The
22 present paper introduces a modification of the maximum horizontal gradient method to
23 overcome these difficulties. A Function f of the two variables x and y :
24 $f_{(x,y)} = a_1x^2 + a_2y^2 + a_3x^2y^2 + a_4x^2y + a_5xy^2 + a_6xy + a_7x + a_8y + a_9$ is established by
25 Gaussian elimination method base on a 3x3 neighborhood data grid. An extract creates a 4-
26 dimensional space based on 4 specific cases of function f , including $x = 0$, $y = 0$, $y = -x$ and y
27 $= x$, they are four functions of one variable. The extreme points position are detected from
28 these functions of one variable. To prove the proposed theoretical basis, as well as the built
29 computer program, the paper presents two numerical models. The obtained results shown that
30 the new approach has more maxima points than the traditional approach. Beside advantages
31 of new approach, some disadvantages is also discussed in this paper. Moreover, we conclude
32 with the application of our new approach to gravitational data in the East Vietnam Sea and
33 demonstrate that we thereby disclose the existence of a gravity trench undetectable in the
34 traditional method.



35 1. Introduction

36 We have many the methods, as well as the approach, can estimate geological
37 boundaries. These methods studied very detailed from the theoretical basis to the numerical
38 models and applied for the real data. In these methods, firstly, we mentioned to the
39 normalized full gradient of gravity anomaly method (NFG) of Berezkin, W.M, 1967 [5].
40 After that, it is applied, improved and developed by the scientists such as:
41 Karsli.H.,Bayrak.Y., 2010[16], Oruc B.,2008, 2012[18,19], Ebrahimzadeh Ardestani. V,
42 2004[10], Ekinci, Y.L., [11,13], Aghajani.H, 2009[1], Sheng.Z,2015 [25]. The horizontal
43 gradient method of Cordell, 1979 [8]. The maximum horizontal gradient method of Blakely,
44 R, J., Simpson, R.W, 1986 [6] and Cordell. L, Grauch. V. J. S, 1985[7]. Using two-variables
45 function to detect the extreme points of Phillips, J.D. 2007[24],...Or the methods use the
46 components of gradient tensor (analytic signal, directional derivatives,...) to approximate
47 geological boundaries and estimate depth simultaneously, such as: Beiki M, (2010,2011
48 [2,3,4]), Ekinci, Y.L., [11,12, 13], Pedersen L.B, 1990 [23], Oruc, B., 2012, 2013 [20,21],
49 Kim Dung N., 2016 [17],... Each author, as well as each method, has the different approach,
50 but the common goal is detect geological boundaries and increase the accuracy of method.
51 These methods are very powerful. They confirmed on many papers and projects of authors,
52 applied for the geological structure research, oil and gas exploration and exploitation, mineral
53 resources on the world.

54 However, each method has advantages and disadvantages. In this paper, we only
55 discuss about the method of Blackely, R. J., Simpson, R.W, 1986 [6] and the method of
56 Phillips, J.D. 2007 [24]. In the method of Blackely,R.J, the limit of method can only detect
57 the maxima point that lies on four dimensions and is the maximum point of a quadratic
58 function that is established by three points on a straight line. Thus, the accuracy of the
59 approximated geological boundaries aren't high enough. In the method of Phillips, J.D,
60 Function of two variables is established base on a 3x3 neighborhood data grid and used to
61 detect the maximum point. Therefore, the maximum point isn't only lies on four dimensions
62 such as the method of Blackely, R. J.,but also can lies anywhere within 3x3 grid points, it is
63 advantage of this method. Nevertheless, the coefficients determination for quadratic surface
64 of Phillips, J.D have unstable accuracy because the equation number is nine whereas the
65 variable number (the coefficient number) is six, thus, it isn't unique root. For these reasons,
66 originating from two-variables function, the paper proposes a new approach, a algorithm that
67 use Gauss elimination method to determine the coefficients of two-variables function base on
68 a 3x3 neighborhood data grid, it holds the geophysics characteristic. Using Gauss elimination



69 method is the marked differences between our approach and Phillips, J.D's approach. After
 70 two-variables function is established, the paper examine four specific cases, including $x=0$,
 71 $y=0$, $y=-x$ and $y=x$, they correspond with four functions of one variable. These functions are
 72 very different from the functions that the proposed Blakely, R, J.,. The maxima points are
 73 detected from these functions.

74

75 **2. Method**

76 The paper researches a function of two variables that has pattern:

77
$$f_{(x,y)} = a_1x^2 + a_2y^2 + a_3x^2y^2 + a_4x^2y + a_5xy^2 + a_6xy + a_7x + a_8y + a_9; \quad (1)$$

78 To determine coefficients a_i of function $f_{(x,y)}$ (1), we use Gauss elimination method.
 79 Namely, from function $f_{(x,y)}$, we can write 9 equations that correspond with 9 data points (3x3
 80 data grid), including: ij^{th} point and 8 neighborhood points (Fig.1):

81 - 1st point: $a_1x_1^2 + a_2y_1^2 + a_3x_1^2y_1^2 + a_4x_1^2y_1 + a_5x_1y_1^2 + a_6x_1y_1 + a_7x_1 + a_8y_1 + a_9 = g_1; (2)$

82

83 - 9th point: $a_1x_9^2 + a_2y_9^2 + a_3x_9^2y_9^2 + a_4x_9^2y_9 + a_5x_9y_9^2 + a_6x_9y_9 + a_7x_9 + a_8y_9 + a_9 = g_9; (3)$

84 In which, $x_1 \div x_9$ and $y_1 \div y_9$ are co-ordinate (x,y) of data points from 1 to 9. For these
 85 equations, we can build the supplemental matrix in the form:

86
$$A_{bs} = \begin{pmatrix} x_1^2 & y_1^2 & x_1^2y_1^2 & x_1^2y_1 & x_1y_1^2 & x_1y_1 & x_1 & y_1 & 1 & g_1 \\ x_2^2 & y_2^2 & x_2^2y_2^2 & x_2^2y_2 & x_2y_2^2 & x_2y_2 & x_2 & y_2 & 1 & g_2 \\ x_3^2 & y_3^2 & x_3^2y_3^2 & x_3^2y_3 & x_3y_3^2 & x_3y_3 & x_3 & y_3 & 1 & g_3 \\ x_4^2 & y_4^2 & x_4^2y_4^2 & x_4^2y_4 & x_4y_4^2 & x_4y_4 & x_4 & y_4 & 1 & g_4 \\ x_5^2 & y_5^2 & x_5^2y_5^2 & x_5^2y_5 & x_5y_5^2 & x_5y_5 & x_5 & y_5 & 1 & g_5 \\ x_6^2 & y_6^2 & x_6^2y_6^2 & x_6^2y_6 & x_6y_6^2 & x_6y_6 & x_6 & y_6 & 1 & g_6 \\ x_7^2 & y_7^2 & x_7^2y_7^2 & x_7^2y_7 & x_7y_7^2 & x_7y_7 & x_7 & y_7 & 1 & g_7 \\ x_8^2 & y_8^2 & x_8^2y_8^2 & x_8^2y_8 & x_8y_8^2 & x_8y_8 & x_8 & y_8 & 1 & g_8 \\ x_9^2 & y_9^2 & x_9^2y_9^2 & x_9^2y_9 & x_9y_9^2 & x_9y_9 & x_9 & y_9 & 1 & g_9 \end{pmatrix} \quad (4)$$

87 If we use local coordinate system and consider $g_{(i,j)}$ point (5th point on Fig.1) is
 88 coordinate origin (coordinate (0,0)) and the distance between two data points on datum line
 89 ox is Δx , on datum line oy is Δy . Put them into matrix (4) and using Gauss elimination
 90 method, we will obtain a triangle matrix:



$$91 \quad A_{bx} = \begin{pmatrix} \Delta x^2 & \Delta y^2 & \Delta x^2 \Delta y^2 & \Delta x^2 \Delta y & -\Delta x \Delta y^2 & -\Delta x \Delta y & -\Delta x & \Delta y & 1 & g_1 \\ 0 & \Delta y^2 & 0 & 0 & 0 & 0 & 0 & \Delta y & 1 & g_2 \\ 0 & 0 & -\Delta x^2 \Delta y^2 & -\Delta x^2 \Delta y & \Delta x \Delta y^2 & \Delta x \Delta y & 2\Delta x & 0 & 1 & g_6 - g_1 + g_2 \\ 0 & 0 & 0 & -2\Delta x^2 \Delta y & 2\Delta x \Delta y^2 & 0 & 2\Delta x & -2\Delta y & 0 & g_9 - g_1 \\ 0 & 0 & 0 & 0 & -2\Delta x \Delta y^2 & 2\Delta x \Delta y & -2\Delta x & 0 & 0 & g_7 - g_9 \\ 0 & 0 & 0 & 0 & 0 & 4\Delta x \Delta y & 0 & 0 & 0 & g_3 - g_1 + g_7 - g_9 \\ 0 & 0 & 0 & 0 & 0 & 0 & -2\Delta x & 0 & 0 & g_4 - g_6 \\ 0 & 0 & 0 & 0 & 0 & 0 & 0 & -2\Delta y & 0 & g_8 - g_2 \\ 0 & 0 & 0 & 0 & 0 & 0 & 0 & 0 & 1 & g_5 \end{pmatrix}; \quad (5)$$

92 From triangle matrix (5), we can infer coefficients a_i as follows:

$$93 \quad a_9 = g_5; \quad a_8 = \frac{g_8 - g_2}{-2\Delta y}; \quad a_7 = \frac{g_4 - g_6}{-2\Delta x}; \quad a_6 = \frac{(g_3 - g_1) + (g_7 - g_9)}{4\Delta x \Delta y};$$

$$94 \quad a_5 = \frac{(g_7 - g_9) + 2(g_6 - g_4) + (g_1 - g_3)}{-4\Delta x \Delta y^2}; \quad a_4 = \frac{(g_9 - g_3) + 2(g_2 - g_8) + (g_7 - g_1)}{-4\Delta x^2 \Delta y};$$

$$95 \quad a_3 = \frac{2(g_8 + g_2) + 2(g_6 + g_4) - (g_7 + g_1) - (g_9 + g_3) - 4g_5}{-4\Delta x^2 \Delta y^2};$$

$$96 \quad a_2 = \frac{g_2 - 2g_5 + g_8}{2\Delta y^2}; \quad a_1 = \frac{g_4 - 2g_5 + g_6}{2\Delta x^2}; \quad (6)$$

97 Therefore, the function of two variables $f_{(x,y)}$ is established for 9 data points (a 3x3
 98 data grid). If we compare this paper's approach with Blackely's approach, we have a
 99 summary table (table 1).

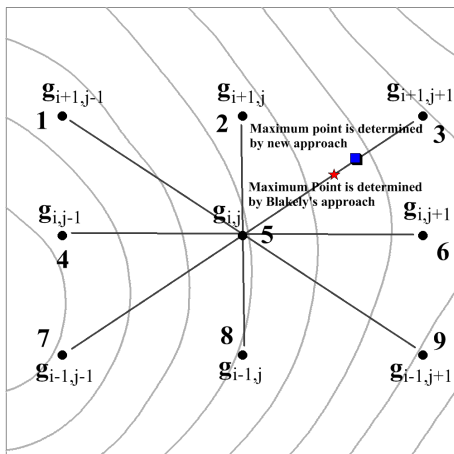


Fig.1. Location of grid intersections
 detect a maximum point near $g_{(i,j)}$.

	Blakely R.J	This paper
The number of equations	4	4
The order of polynomial	2	2 (for case: $x=0, y=0$); and 4 (for case: $y=-x, y=x$)
Determine the coefficients of function	Base on 3 points	Base on 9 points
Detect the maximum point	- ij^{th} point is larger 2 surround points (straight line)	- the extreme point is larger 2 surround points (straight line)

Table.1. Compare Blakely's problem with
 problem of this paper

100 To detect the maxima points of function $f_{(x,y)}$. Firstly, we have to detect the critical
 101 points (may be maximum point, minimum point, saddle point) by the simultaneous solution of



102 equations $f_x = 0; f_y = 0$. Secondly, applying the extreme conditions of two-variables
 103 function to detect maximum point. However, this paper doesn't detect the critical points from
 104 function $f_{(x,y)}$ but detects the extreme points from 4 functions of one variable that
 105 corresponds with 4 specific cases of function $f_{(x,y)}$ (cases: $x=0, y=0$, $y=-x$ and $y=x$, view
 106 equations from A-2 to A-5 (Appendix A)). Locate of the maximum point on each dimension,
 107 along with the corresponded condition, is determined by the expression A-8, A-9, A-12, A-13
 108 and A-18 to A-21 (Appendix A).

109 Base on the proposed theoretical basis, we built a computer program by the Matlab
 110 computer programming language to detect the extreme points on 4 dimensions.

111

112 **3. Test cases**

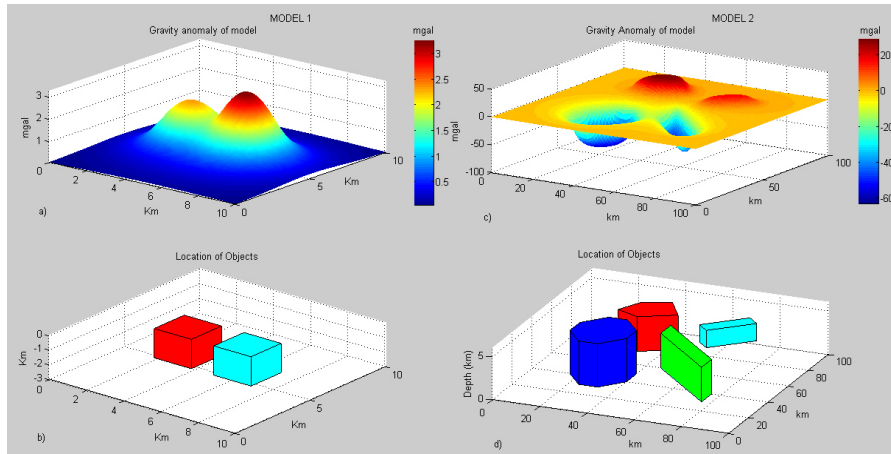
113 Hereafter, the paper use the built computer program to test on two numerical model.
 114 The parameters of each model are given in the *table 2* and are shown on *figure 2*. In which,
 115 the model 1 has two objects, the points number on datum-line ox and datum-line oy: $n_x=101$,
 116 $n_y=101$, the distance between points on both ox and oy: $dx=0.1\text{km}$, $dy=0.1\text{km}$. The model 2
 117 has four objects, the points number on datum-line ox and datum-line oy: $n_x=101$, $n_y=101$, the
 118 distance between points on both ox and oy: $dx=1\text{km}$, $dy=1\text{km}$. The gravity anomaly, as well
 119 as the location of objects, is created and calculated by a Matlab code that is built base on the
 120 theoretical basis of Mantik Talwni and Maurice Ewing [26].

121

	Model 1			Model 2		
	Points location xi/yi (km)	Depth z1/z2 (km)	Density constrast (g/cm ³)	Points location xi/yi (km)	Depth z1/z2 (km)	Density constrast (g/cm ³)
Object 1	2.4/4 ; 2.4/6 ; 4.4/6; 4.4/4	0.5/2.5	0.1	24/69 ; 29/80 ; 40/85; 48/72 ; 34/64 ; 24/69	1/5	0.1
Object 2	5.6/4 ; 5.6/6 ; 7.6/4 ;7.6/6	0.5/2.5	0.15	20/30 ; 20/40 ; 28/50 ; 36/50; 44/40 ; 44/30 ; 36/20 ; 28/20	1/6	-0.2
Object 3				60/65; 75/80; 80/75; 65/60	3/5	0.1
Object 4				50/50; 50/60; 80/30; 80/20	1/5	-0.2

122

Table 2: The parameters of two models

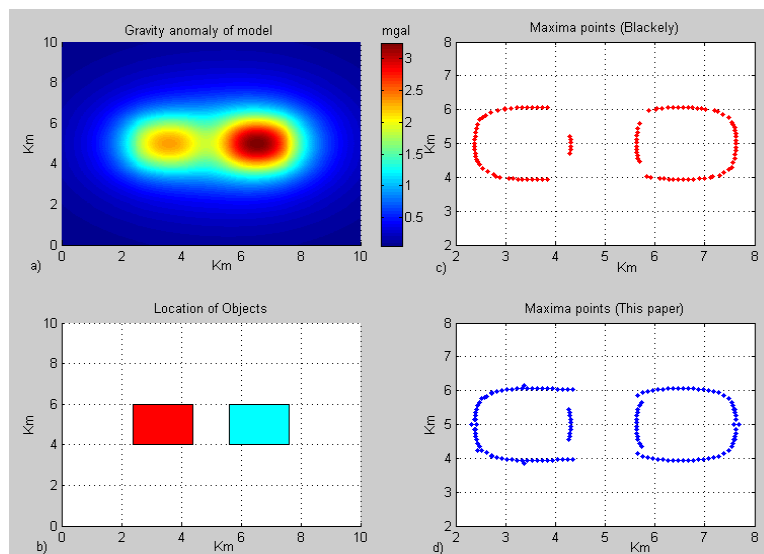


123
 124 *Fig 2: a). Gravity anomaly of objects for model 1; b). Location of objects for model 1;*
 125 *c). Gravity anomaly of objects for model 2; d). Location of objects for model 2;*

126 **3.1. Model 1:**

127 **3.1.1. Case 1: The model hasn't noise.**

128 Firstly, the paper test on model hasn't noise, it has only anomaly of objects (*figure 2a,*
 129 *3a*). The maxima points are detected from the horizontal gradient amplitude function of
 130 gravity anomaly by both approaches. The results are presented in *figure 3*. With the red points
 131 are the result from Blakely's approach (*fig.3c*) and the blue points are the result from new
 132 approach (*fig.3d*).



133
 134 *Figure 3: The results of model hasn't noise .*



135 From the figure shown that the blue point is more than the red point. Namely, for
 136 object 1, at $x > 4$ km, the red point exists little, whereas, the blue point exists more. A
 137 similarity for object 2, at $x < 6$ km, we can also see the blue point is still more than the red point
 138 *3.1.2. Case 2: The model has noise.*

139 To insert the noise into the model data. The author use fomular below (values from
 140 the uniform distribution on the interval $[a, b]$):

141 Noise_Insert = $a + (b - a) \cdot \text{rand}(n, 1)$; with: $n = \text{length}(\text{data})$;

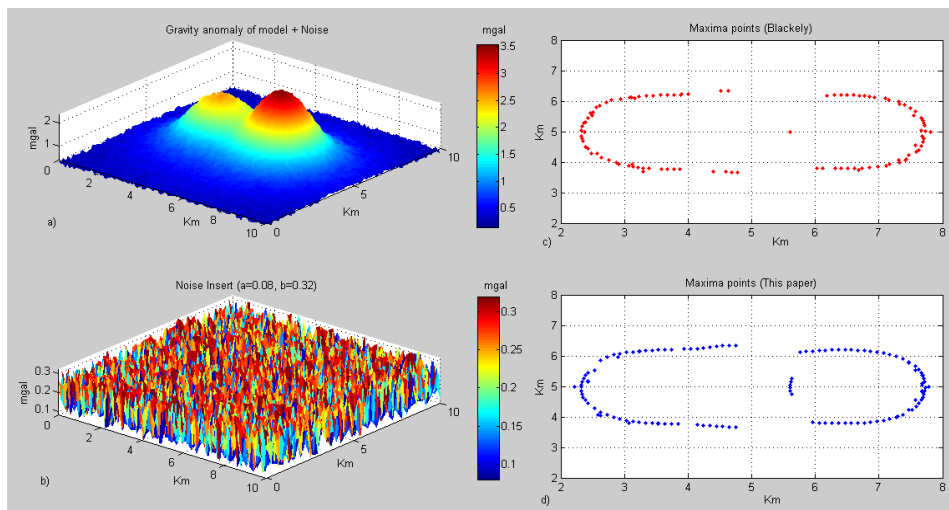
142 The paper test for case : $a = 0.08$, $b = 0.32$.

143 then: Data_have_noise = model data + Noise_Insert.

144 A upward continuation was processed to attenuate the effect of the shortest
 145 wavelengths:

146
$$Up(x, y) = F^{-1} \left\{ \left(e^{-\Delta z |k|} \right) F(g) \right\}; \text{ with } \Delta z = 0.5 \text{ (km)}.$$

147 The maxima points are detected from the horizontal gradient amplitude function of
 148 the upward continued field by both approaches. The results are shown on *fig. 4*. With the red
 149 points are the result from Blakely's approach and the blue points are the result of new
 150 approach.



151
 152 *Figure 4: The model has noise (with $a = 0.08$, $b = 0.32$)*

153 From the figure, we can see that the noise is still appear on both results (some the
 154 maxima points appear on edge). It can be explained due to a 0.5 km upward continuation
 155 process can't remove the perfect noise. However, we can see the blue point is more than the
 156 red point. Namely, for object 1, at $x > 4$ km, the blue point is more than the red point. For



157 object 2, at $x < 6$ km, the red point almost no exist (only one point) but the blue point still
158 appears. The boundaries of two objects can be approximated by these maxima points.
159 Therefore, if we use the blue points to approximate the edge of objects, it will show more
160 clearly in the both cases, has and hasn't noise

161 * *Comments:* From the results obtained on this model shown:

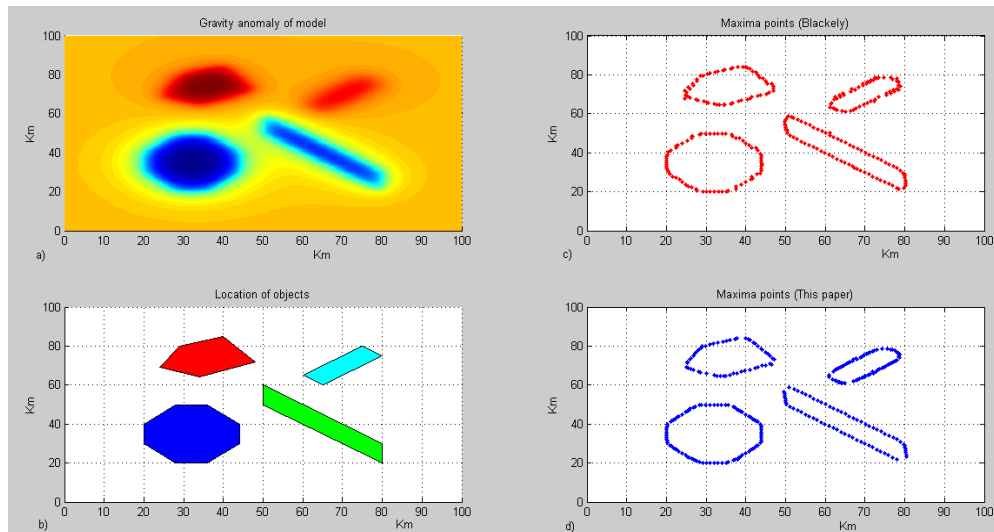
162 - The proposed theoretical basis in this paper, as well as the built computer program
163 by this theory, is correct and logical. This is a new approach, a algorithm that can use to
164 detect the edge points of objects by the potential field data.

165 - The maxima points are detected by this algorithm are more than Blakely's approach
166 in the both case, hasn't noise and has noise.

167

168 3.2. Model 2

169 3.2.1. Case 1: The model hasn't noise.



170

171

Figure 5: The results for model 2. Case hasn't noise

172 The same model 1, the paper also test two case: hasn't noise and has noise. This
173 model has 4 objects, they are right prisms with the top and the bottom are polygons (*fig.2d*
174 *and fig.5b*).

175 For model 1, both case, to detect the maximum point from the extreme points, the
176 paper can choose $n \geq 2$ (satisfying equations number). But for model 2, in this case, if we
177 choose $n \geq 2$, it is loosely. Therefore, the paper chose $n > 2$ for the new approach (*figure 5d*)
178 and $n \geq 2$ for Blackely's approach (*figure 5c*).

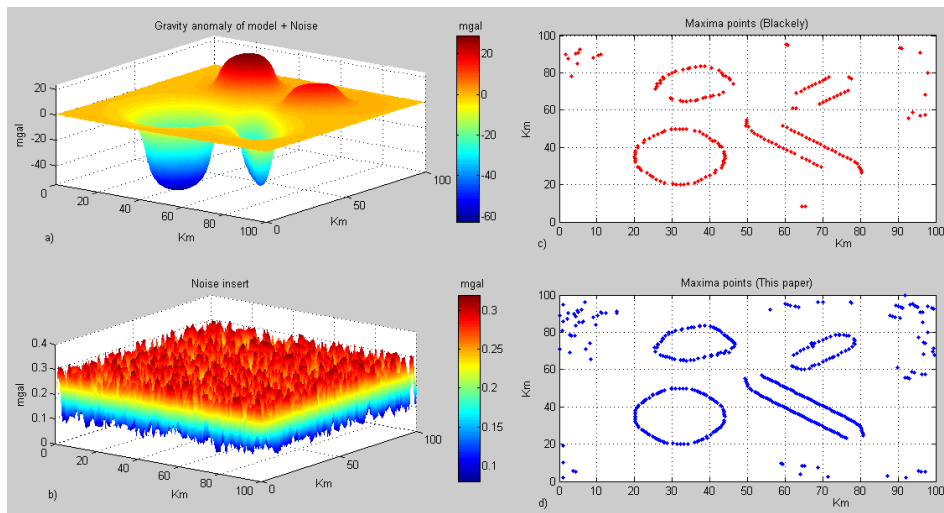


179 3.2.2. Case 2: The model has noise.

180 The same model 1, the paper also insert noise by formular:

181 Noise_Insert = a+(b-a).*rand(n,1); with a=0.08, b=0.32, n=length(data);

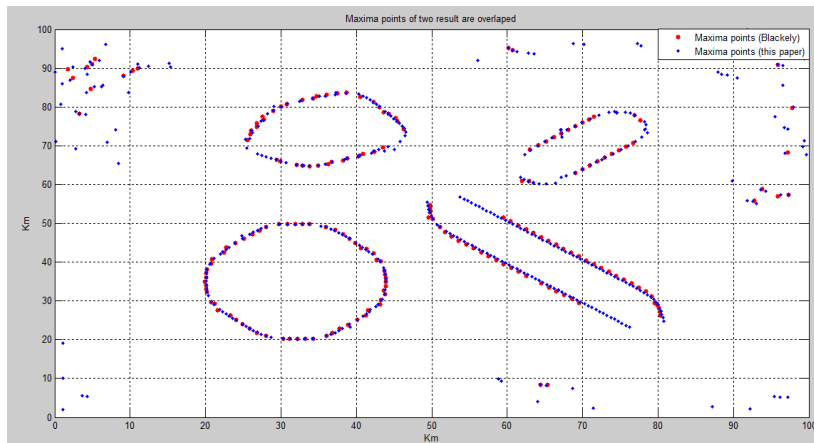
182 A 1.5km upward continuation was processed to attenuate the effect of the shortest
 183 wavelengths. In this case, the paper chose $n > 2$ for both the new approach and Blackely's
 184 approach. The obtained results are shown on figure 6c and 6d.



185

186

Figure 6: The results for model 2. Case has noise



187

188

Fig 7: The maxima points of two results are overlaped

189 * Comments:

190 - Confirmation: From the results are tested on model 2, one again shown that the
 191 proposed theoretical basis in this paper, as well as the computer program is built base on this



192 theory, is correct and logical. It is used to detect the maxima points (the edge points of
193 objects) and approximate the geological boundaries.

194 - *Advantage*: Zoom in and view the results on *figures 5c, 5d* and *figure 6c, 6d* and
195 *figure 7*, we can see that the maxima points order are detected by new approach are more
196 stable, more near at the real edge than Blakely's approach. Therefore, using the blue points to
197 approximate the edge of objects will show more clearly in both case.

198 - *Disadvantage*: It is selection $n \geq 2$. For model 1, we can choose $n \geq 2$ for both
199 approaches. But for model 2, with the new approach, if we choose $n \geq 2$, it is loose. Therefore,
200 the paper chose $n > 2$ for both cases (hasn't noise and has noise). In the case has noise, it is
201 more tight, has more points than the Blackely's approach (*fig. 7*).

202

203 4. Real data application

204 Hereafter, the paper presents the results of the application of our new approach to
205 detect the maxima points of the horizontal gradient amplitude function of the second vertical
206 derivative of the gravity field and approximate the structural boundaries by the bouguer
207 gravity anomaly data in the East Vietnam Sea that is directly calculated from Free-air gravity
208 anomaly data [27] and seabed topography [27] by Parker's algorithm [22], both data sources
209 have scale 1minute.

210 The application area has the coordinate: $108^{\circ}\text{E}-116^{\circ}\text{E}$, $6^{\circ}\text{N}-18^{\circ}\text{N}$. The bouguer gravity
211 anomaly on research area has the fluctuation value from -35mgal to 325mgal .

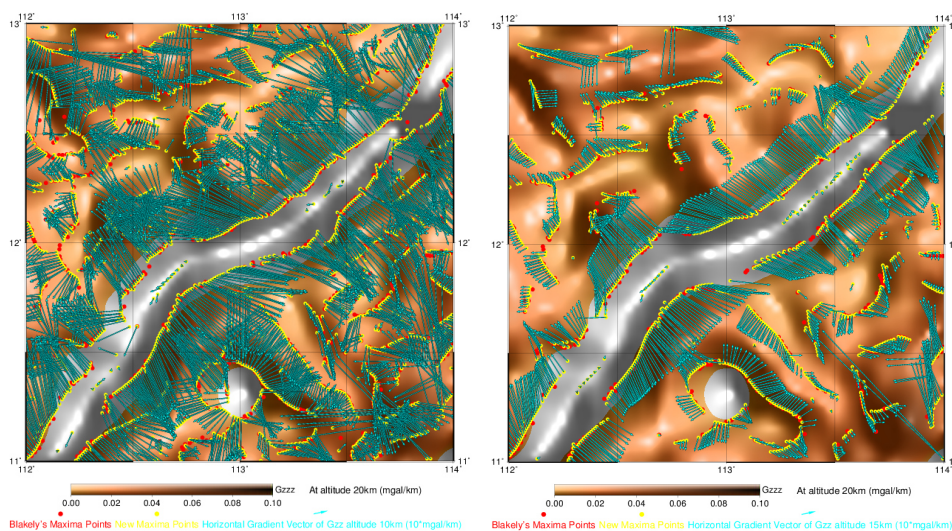
212 The gravity field g which is measured by gravimeter varies with height, that is, there
213 is vertical gradient g_z . Over a non-uniform earth in which density varies laterally, the vertical
214 changes and the rate of change g_{zz} is thus the second vertical derivative of the gravity field g_z .

215 Therefore, from the bouguer gravity anomaly, the paper make the upward
216 continuation at other altitudes, including: 10, 15, 20, 25, 30km. These calculative steps can
217 remove a great part of the residual anomalies (the effect of the shortest wavelengths) that is
218 caused by the seabed terrain or the local geology structures [15]. Each these upward
219 continued gravity fields is calculated the first vertical derivative. Each fields obtained after
220 derivation is used to calculate the horizontal gradient and the horizontal gradient amplitude.
221 The maxima points are detected from these horizontal gradient amplitude fields by both
222 approach (choose $n \geq 2$ for both). The obtained results are shown on figures *8a, 8b, 8c, 8d,*
223 *8e, 8f* and *9*.

224 Figures (*figure 8a, 8b, 8c, 8d, 8e, 8f*) that a part of results is zoomed in for we can view
225 more detailer about the difference between results of two approach at other altitudes. In



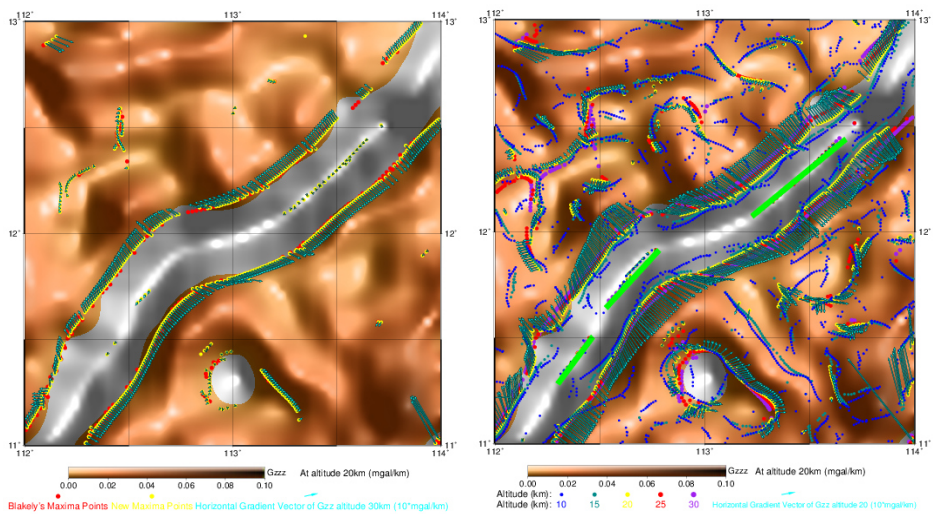
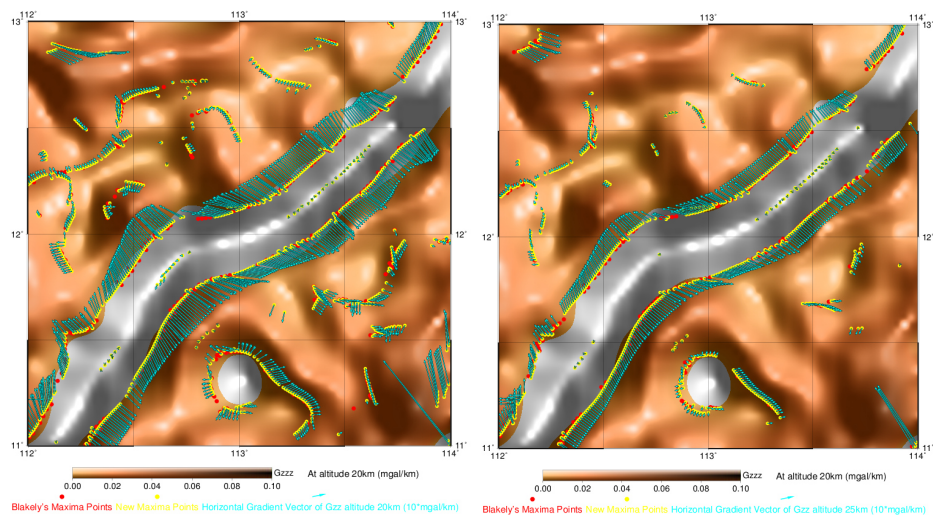
226 which, the yellow points are detected by our approach, the red points are detected by
227 Blackely's approach and the horizontal gradient vectors are shown by the cyan color (the
228 amplitude is multiplied with 10). We can see that many points (yellow points) are detected
229 by our new approach but aren't detected by Blackely's approach at any altitudes. There, their
230 horizontal gradient vectors have small amplitude and quite confusional direction. These
231 maxima points are approximated by the green polylines (*Fig. 8f*). We believe that the green
232 polylines are a new boundary because it wasn't shown in the projects and articles [9, 14].
233 This boundary is only detected base on our algorithm by the bouguer gravity anomaly. In the
234 future, this boundary can be verified by the other geophysics methods, as well as other
235 geology results.
236



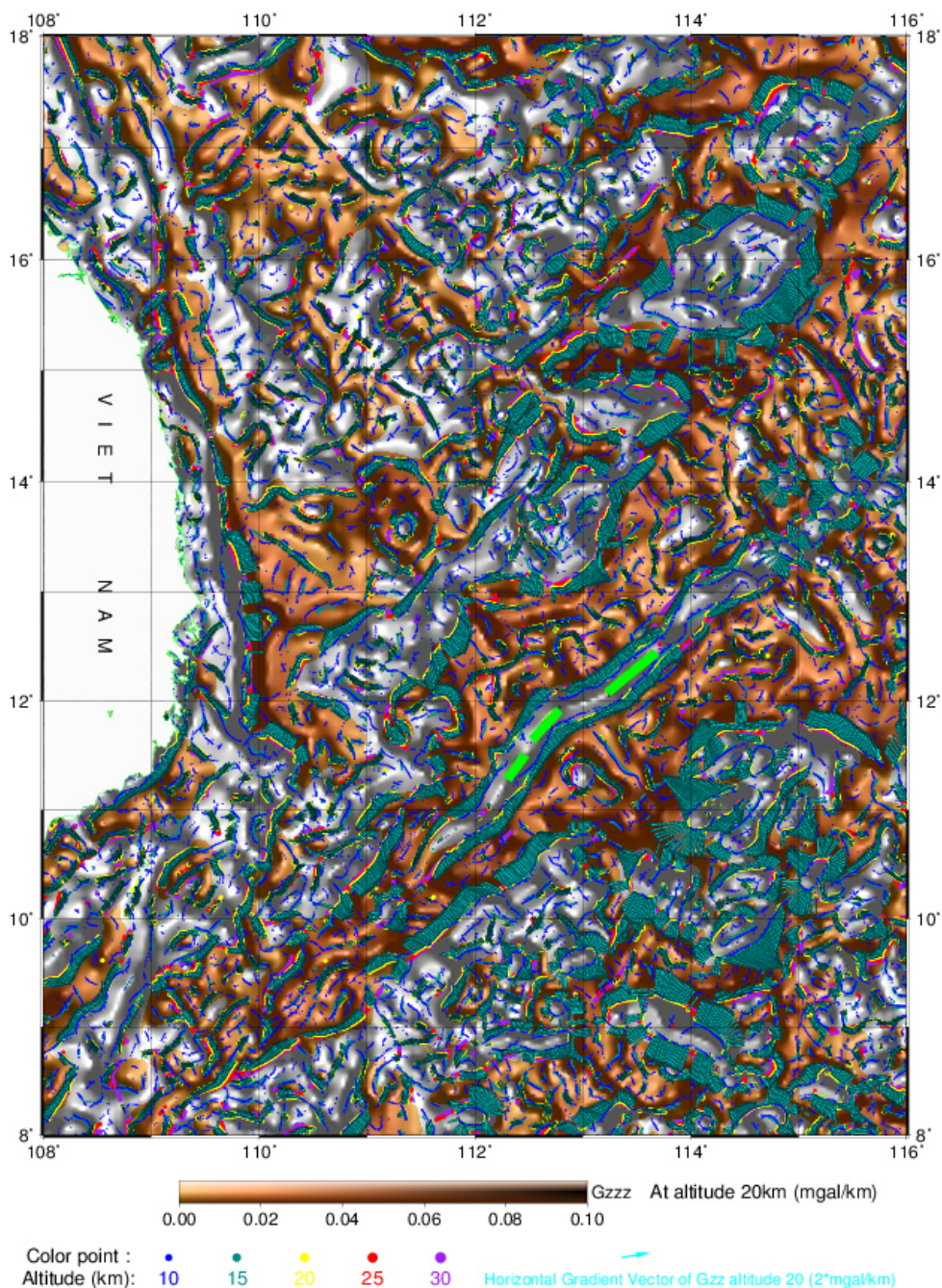
237

Figure 8a). Altitude 10 km

Figure 8b). Altitude 15 km



240 The maxima points that are detected at other altitudes base on our new approach in
 241 the East Vietnam Sea are shown on figure 9



242

243

244

245

Figure 9. The maxima points are detected base on new approach by the bouguer gravity anomaly in the East Vietnam Sea (the green polylines are the approximated boundaries that is only detected by our approach)



246 **5. Conclusion**

247 Originating from two-variables function that the coefficients are established by Gauss
248 elimination method base on 9 data points and examine on their specific cases (including: case
249 $x=0$, $y=0$ correspond with two quadratic functions, case $y=-x$, $y=x$ correspond with two
250 quartic functions) the paper proposed a the theoretical basis, a algorithm to detect the maxima
251 points.

252 Base on the theoretical basis that the paper proposed, the paper built a computer
253 program by the Matlab computer programming language to detect the extreme points, the
254 maximum point on 4 dimensions correspond with 4 functions of one variable. From the
255 results tested on the numeric models shown that the built computer program, as well as the
256 proposed theoretical basis, is correct and logical.

257 From the results obtained on the numeric models and applied on real data shown that
258 the maxima points are detected by new approach have more points than Blakely's approach.
259 Therefor, Using the maxima points are detected by new approach to approximate the edge of
260 objects are better.

261 We conclude with the application of our new approach to gravitational data in the
262 East Vietnam Sea and demonstrate that we thereby disclose the existence of a gravity trench
263 undetectable in the traditional method.

264
265
266
267
268
269
270
271
272
273
274
275
276
277
278
279



280

APPENDIX A

281

Solving the specific cases of two-variables function

282

283 1). The specific cases of two-variables function

284 $f_{(x,y)} = a_1x^2 + a_2y^2 + a_3x^2y^2 + a_4x^2y + a_5xy^2 + a_6xy + a_7x + a_8y + a_9;$ (A-1)

285 * Case: $x=0:$ $f_{(x,y)}^{x=0} = a_2y^2 + a_8y + a_9;$ (A-2)

286 * Case: $y=0:$ $f_{(x,y)}^{y=0} = a_1x^2 + a_7x + a_9;$ (A-3)

287 * Case: $y=-x:$ $f_{(x,y)}^{y=-x} = a_3x^4 + (a_5 - a_4)x^3 + (a_1 + a_2 - a_6)x^2 + (a_7 - a_8)x + a_9;$ (A-4)

288 *Case: $y=x:$ $f_{(x,y)}^{y=x} = a_3x^4 + (a_5 + a_4)x^3 + (a_1 + a_2 + a_6)x^2 + (a_7 + a_8)x + a_9;$ (A-5)

289 To detect the extreme points of these cases, we have to calculate the first-order
 290 derivative these functions (equation A-2, A-3, A-4,A-5) and solve these:

291 * Case: $x=0:$ $2a_2y + a_8 = 0$ (A-6)

292 therefore: $y_m = \frac{-a_8}{2a_2}$; and replace into equation A-2, we obtain:

293 $g_{\max}^{x=0} = a_2y_m^2 + a_8y_m + a_9;$ (A-7)

294 if: $-dy < y_m = \frac{-a_8}{2a_2} < 0;$ and $g_8 \leq g_{\max}^{x=0} \geq g_5;$ (call is segment 8-5); (A-8)

295 if: $0 < y_m = \frac{-a_8}{2a_2} < dy;$ and $g_2 \leq g_{\max}^{x=0} \geq g_5;$ (segment 2-5); (A-9)

296 * Case: $y=0:$ $2a_1x + a_7 = 0$ (A-10)

297 therefore: $x_m = \frac{-a_7}{2a_1}$, and replace into eq. A-3, we obtain: $g_{\max}^{y=0} = a_1x_m^2 + a_7x_m + a_9;$ (A-11)

298 if: $-dx < x_m = \frac{-a_7}{2a_1} < 0;$ and $g_4 \leq g_{\max}^{y=0} \geq g_5;$ (segment 4-5); (A-12)

299 if: $0 < x_m = \frac{-a_7}{2a_1} < dx;$ and $g_6 \leq g_{\max}^{y=0} \geq g_5;$ (segment 6-5); (A-13)

300 * Case: $y=-x:$ $4a_3x^3 + 3(a_5 - a_4)x^2 + 2(a_1 + a_2 - a_6)x + (a_7 - a_8) = 0$ (A-14)



301 With

$$\begin{aligned} a &= 4a_3; \\ b &= 3(a_5 - a_4); \\ c &= 2(a_1 + a_2 - a_6); \\ d &= a_7 - a_8; \end{aligned}$$

302 We obtain: $ax^3 + bx^2 + cx + d = 0;$ (A-15)

303 * **Case: $y=x$:** $4a_3x^3 + 3(a_5 + a_4)x^2 + 2(a_1 + a_2 + a_6)x + (a_7 + a_8) = 0;$ (A-16)

304 With

$$\begin{aligned} a &= 4a_3; \\ b &= 3(a_5 + a_4); \\ c &= 2(a_1 + a_2 + a_6); \\ d &= a_7 + a_8; \end{aligned}$$

305 We obtain: $ax^3 + bx^2 + cx + d = 0;$ (A-17)

306 To solve equations (A-15 and A-17) we use *Appendix below: 2). Solving cubic*
 307 *equation*

308 The roots $x_m^{y=-x}$ (case $y=-x$) and $x_m^{y=x}$ (case $y=x$) are determined by expression
 309 from A-25 to A-27 or A-28 or A-29 or A-30.

310 Case $y=-x$, we will have $y_m=-x_m$. Replace $(x_m^{y=-x}, y_m)$ into (A-4) we have $g_{\max}^{y=-x}$

311 Case $y=x$, we will have $y_m=x_m$. Replace $(x_m^{y=x}, y_m)$ into (A-5) we have $g_{\max}^{y=x}$

312 Now, we examine:

313 if: $-dx < x_m^{y=-x} < 0;$ and $g_1 \leq g_{\max}^{y=-x} \geq g_5;$ (call is segment 1-5); (A-18)

314 if: $0 < x_m^{y=-x} < dx;$ and $g_9 \leq g_{\max}^{y=-x} \geq g_5;$ (segment 9-5); (A-19)

315 if: $-dx < x_m^{y=x} < 0;$ and $g_7 \leq g_{\max}^{y=x} \geq g_5;$ (segment 7-5) (A-20)

316 if: $0 < x_m^{y=x} < dx;$ and $g_3 \leq g_{\max}^{y=x} \geq g_5;$ (segment 3-5); (A-21)

317 Like this, we have 4 directions and are separated into 8 segments. To have a
 318 maximum point, we need choose $n \geq 2$ (conditional satisfiable segments on total 8 segments
 319 (A-8, A-9, A-12, A-13 and A-18 to A-21)).

320

321 **2). Solving cubic equation**

322 Supposing that we have a cubic equation:

323 $ax^3 + bx^2 + cx + d = 0;$ (with a $\neq 0$) ; (A-22)

324 $\Delta = b^2 - 3ac$ (A-23)



$$k = \frac{9abc - 2b^3 - 27a^2d}{2\sqrt{|\Delta|^3}} \quad (\text{A-24})$$

1). If $\Delta > 0$ and $|k| \leq 1$, equation (A-22) has 3 roots:

$$x_1 = \frac{2\sqrt{\Delta}\cos\left(\frac{\arccos(k)}{3}\right) - b}{3a}; \quad (\text{A-25})$$

$$x_2 = \frac{2\sqrt{\Delta}\cos\left(\frac{\arccos(k)}{3} - \frac{2\pi}{3}\right) - b}{3a}; \quad (\text{A-26})$$

$$x_3 = \frac{2\sqrt{\Delta}\cos\left(\frac{\arccos(k)}{3} + \frac{2\pi}{3}\right) - b}{3a}; \quad (\text{A-27})$$

2). If $\Delta > 0$ and $|k| > 1$, equation (A-22) only has one root:

$$x = \frac{\sqrt{\Delta}|k|}{3ak} \left(\sqrt[3]{|k| + \sqrt{k^2 - 1}} + \sqrt[3]{|k| - \sqrt{k^2 - 1}} \right) - \frac{b}{3a} \quad (\text{A-28})$$

3). If $\Delta = 0$, equation (A-22) has multiples roots:

$$x = \frac{-b + \sqrt[3]{b^3 - 27a^2d}}{3a}; \quad (\text{A-29})$$

4). If $\Delta < 0$, equation (A-22) only has one root

$$x = \frac{\sqrt{|\Delta|}}{3a} \left(\sqrt[3]{k + \sqrt{k^2 + 1}} + \sqrt[3]{k - \sqrt{k^2 + 1}} \right) - \frac{b}{3a} \quad (\text{A-30})$$

336
 337
 338

339 Acknowledgements

340 The author sincerely thank for the projects of VAST (code: QTRU02.01/19-20,
 341 QTRU02.01/20-21, VAST06.01/20-21) and KHCBTĐ.02/18-20 project, VT-UD.04/17-20
 342 project supported conditions for complete this paper.

343
 344
 345
 346
 347



348 **References**

- 349 [1]. Aghajani.H, Ali Moradzadeh and Hualin Zeng (2009), “ Normalized full gradient of
350 gravity anomaly method and its application to the mobrun sulfide body, Canada”, *World*
351 *applied sciences journal*, Vol.6(3), pp.393-400.
- 352 [2]. Beiki M. (2010), “Analytic signals of gravity gradient tensor and their application to
353 estimate source location”, *Geophysics*, Vol.75(6), pp.159-174.
- 354 [3]. Beiki M. (2011), *New techniques for estimation of source parameters. Application to*
355 *airborne gravity and pseudo-gravity gradient tensors*. Acta Universitatis Upsaliensis.
356 Digital comprehensive summaries of Uppsala dissertation from the faculty of science
357 and technology 730. 80 pp. Uppsala. ISBN 978-91-554-7986-2.
- 358 [4]. Beiki M., Pedersen L.B. (2010), “Eigenvector analysis of gravity gradient tensor to locate
359 geologic bodies”, *Geophysics*, Vol.75(6), pp.137–149.
- 360 [5]. Berezkin.W.M.(1967), “Application of the full vertical gravity gradient to determination
361 to sources causing gravity anomalies (in Russian)”, *Expl. Geopys.*,18,pp.69-76.
- 362 [6]. Blakely R.J., and R.W.Simpson (1986), “Approximating edges of source bodies from
363 magnetic or gravity anomalies”, *Geophysics*, Vol.51(7), pp.1494–1498, doi:
364 10.1190/1.1442197.
- 365 [7]. Cordell L., Grauch. V. J. S. (1985), “Mapping basement magnetization zones from aero-
366 magnetic data in the San Juan basin, New Mexico. in Hinze. W. J., Ed..The utility of
367 regional gravity and magnetic anomaly maps”, *Sot.Explor.Geophys.*,tr.181-197.
- 368 [8]. Cordell. L. (1979), “Gravimetric expression of graben faulting in Santa Fe country and
369 the Espanola Basin, New Mexico”, *New Mexico Geological Society 30th Annual Fall*
370 *Field Conference Guidebook*, pp.59-64.
- 371 [9]. Dung T.T., Que B.C., nnk (2013), “Cenozoic basement structure of the south china sea
372 and adjacent areas by modeling and interpreting gravity data”, *Russian journal of pacific*
373 *geology*, Vol 7, No.4, pp.227-236.
- 374 [10]. Ebrahimzadeh Ardestani, V. (2004), “Detection of near – surface anomalies through 2-
375 D normalized full gradient of gravity data”, *J.Eath&Space Physics*. Vol 30, No.2, 2004,
376 P.1-6
- 377 [11]. Ekinci, Y.L., and Yiğitbaş, E., (2012), “A geophysical approach to the igneous rocks in
378 the Biga Peninsula (NW Turkey) based on airborne magnetic anomalies: geological
379 implications ”, *Geodinamica Acta*, Vol.25, Nos.3-4, p.267-285.
- 380 [12]. Ekinci, Y.L., Ertekin, C., Yiğitbaş, E., (2013), “On the effectiveness of directional
381 derivative based filters on gravity anomalies for source edge approximation: synthetic



- 382 simulations and a case study from the Aegean graben system (western Anatolia,
383 Turkey)”, *Journal of geophysics and engineering*, Vol.10, Issue.3, 035005.
- 384 [13]. Ekinci, Y.L., and Yiğitbaş, E., (2015), “Interpretation of gravity anomalies to delineate
385 some structural features of Biga and Gelibolu peninsulas, and their surroundings (north-
386 west Turkey) ”, *Geodinamica Acta*, Vol.27, No.4, p.300-319.
- 387 [14]. Hiep N., (2005), *Geology and oil resources of Vietnam*, Vietnam Oil and Gas Group,
388 Hanoi.
- 389 [15]. John M. Reynolds, (1997), “*An Introduction to applied and environmental geophysics*”,
390 John Wiley & Sons Ltd, The Atrium, Southern gate, Chichester, West Sussex PO19 8SQ,
391 England.
- 392 [16]. Karsli.H., Bayrak. Y., (2010), “Application of the normalized total gradient method to
393 calculate envelop of seismic reflection signals”, *Journal of Applied Geophysics* 71, p.90-
394 97.
- 395 [17]. Kim Dung N., Thanh D.D., (2016), “Using the analytic signal method of gravity
396 gradient tensor (GGT) to determine the location and depth of the faults in the Pre-
397 Cenozoic basement rocks of the Red River trough”, *Vietnam Journal of Earth Sciences*
398 38 (2), pp.143-152.
- 399 [18]. Oruc B., Keskinsezer A. (2008), ”Structural setting of the Northeastern Biga Peninsula
400 (Turkey) from tilt derivatives of gravity gradient tensors and magnitude of
401 horizontal gravity components”, *Pure Appl. Geophys*, Vol.165, pp.1913–1927.
- 402 [19]. Oruc. B., Keskinsezer A. (2008), “Detection of causative bodies by normalized full
403 gradient of aeromagnetic anomalies from east Marmara region, NW Turkey”, *Journal of*
404 *Applied Geophysics* 65, pp. 39-49.
- 405 [20]. Oruc. B., (2012), “Source Location and Depth Estimation Using Normalized Full
406 Gradient of Magnetic Anomalies”, *Yerbilimleri*, Vol.33 (2), p.177-192
- 407 [21]. Oruc B., Sertcelik I., Kafadar O., Selim H.H., (2013), “Structural interpretation of the
408 Erzurum Basin, eastern Turkey, using curvature gravity gradient tensor and gravity
409 inversion of basement relief “, *J. Appl. Geophys*, Vol. 88, pp.105–113.
- 410 [22]. Pedraza De Marchi A.C., Ghidella M.E., Tocho C. N., “Analysis of different
411 methodologies to calculate bouguer gravity anomalies in the argentine continental
412 margin”, *Geosciences* 2014, 4(2): 33-41.
- 413 [23]. Pedersen L. B., and T. M. Rasmussen (1990), “The gradient tensor of potential field
414 anomalies: Some implications on data collection and data processing of maps”,
415 *Geophysics*, Vol.55, pp.1558–1566, doi: 10.1190/1.1442807.



- 416 [24]. Phillips, J.D., Hansen, R.O. and Blakely, R.J., 2007, *The use of curvature in potential-*
417 *field interpretation*, *Exploration Geophysics*, 38(2), pp.111-119
- 418 [25]. Sheng. Z, Xiaohong.M. (2015), “Improved normalized full-gradient method and its
419 application to the location of source body”, *Journal of Applied Geophysics* 113, pp.86-
420 91.
- 421 [26]. Talwani,. M and Ewing,.M, 1960, “Rapid computation of gravitational attraction of
422 three-dimensional bodies of arbitrary shape”, *Geophysics*, vol.15, No.1, pp.203-225.
- 423 [27]. http://topex.ucsd.edu/cgi-bin/get_data.cgi
- 424 [28]. https://en.wikipedia.org/wiki/Cubic_function
- 425